IMPROVED PRE-CALCULATION OF SOLAR THERMAL PRODUCTION FOR MILP-BASED OPTIMIZATION PROBLEMS

Thibaut Wissocq[1], Nicolas Lamaison[1]

[1] Univ. Grenoble Alpes, CEA, Liten, Campus Ines, 73375 Le Bourget du Lac (France)

Abstract

The decarbonisation of heat supply in district heating network can be achieved through solar thermal systems, providing a carbon-free and competitive energy. Their integration with large-scale thermal storage allows for enhancing solar fraction by utilizing summer heat during winter months. However, conventional optimization tools often treat solar thermal production as a simple input, potentially leading to miscalculations and neglecting the influence of storage behavior on the thermal solar production. The presence of a thermal storage especially influences both the temperature and the mass flow observed by the solar plant. In this context, a good prediction of solar production is crucial for a better computation of the system. We propose here a 6-step methodology based on simulation and optimization models to enhance solar thermal production pre-calculation. With this methodology, the predicted solar production has resulted in an average error of 3.4% compared to the final solar production obtained after convergence of optimization/simulation of the entire plant, on six district heating cases studies. The latter has to be compared with an average error of 10% when using a state-of-the-art approach for the solar production calculation.

Keywords: solar thermal, simulation, Dymola, Modelica, long-term storage, district heating.

1. Introduction

1.1. The role of solar thermal in district heating network

A major part of final energy consumption in European countries is dedicated to space heating and domestic hot water needs. District heating networks (DHNs) have emerged as a promising solution for reducing carbon emissions in heat supply. Notably, the 4th generation of district heating currently under development across Europe, focuses on lower temperature networks compared to older generations (2nd and 3rd generation). This evolution enhances the integration of renewable heat sources, such as heat pumps and solar thermal plants (Lund, 2014).

Solar district heating networks (SDH) are a specific type of district heating system that primarily relies on solar thermal plants as the main source of energy, aiming for a high solar fraction. Solar thermal systems offer several key advantages: they are renewable, carbon-free, and contribute to diversifying energy sources, thereby reducing dependency on fossil fuels and enhancing energy security.

A particularly significant advantages of solar thermal systems is their compatibility with large-scale thermal storage. By coupling solar thermal plants with thermal storage, excess heat generated during the summer months can be stored and then utilized during periods of lower solar availability, such as in the winter. This coupling not only increases the overall efficiency and solar fraction of the system but also ensures a more stable and reliable heat supply throughout the year. The ability to shift energy production across seasons makes solar thermal coupled with storage a particularly attractive option for sustainable district heating networks. The presence of thermal storages can also benefit other production methods by optimizing the overall system efficiency and reducing heat production costs

However, SDH are generally more complex than classical DHN. The inherent intermittency of solar resources adds further complexity to managing SDHs compared to traditional DHNs. Optimizing the operation of solar district heating (SDH) systems presents significant challenges due to the intricate interactions between various components, particularly when thermal storage is involved. Thermal storage operation affects both DHN temperature and mass flow rates. Since solar collectors are sensitive to operating temperatures, the behavior of thermal storage can significantly impact the overall system efficiency. Therefore, a deep understanding of the thermal-hydraulic behavior within these networks is crucial for optimizing their design, operation, and control strategies, to ensure maximum efficiency and reliability. To address these challenges, mathematical tools such as simulation or optimization models can help to address the intricate task of matching demand with supply in district heating networks.1.2. How SDH are modelled in the literature

© 2024. The Authors. Published by International Solar Energy Society
Selection and/or peer review under responsibility of Scientific Committee
10.18086/eurosun.2024.03.09 Available at http://proceedings.ises.org

In the literature, two main methods are used to model solar district heating network. The first approach involves simulation tools such TRNSYS (University of Wisconsin, 1975) or Modelica models (Brück, 2002). These methods employ expert rules such as plant priority settings for energy dispatch and are able to model non-linear equations, thus, offering a more accurate representation of solar production profiles (Giraud., 2014; Descamps, 2018; Renaldi 2019). However, while simulations can enhance the understanding of system behavior, they do not ensure optimal economic or environmental solutions, as thermal plants production profiles are predefined from rules rather than optimization computation. Therefore, optimization methods are often used for optimal dispatch.

Optimization methods involve modeling solar district heating (SDH) equations as constraints to minimize an objective function, which can be economic (e.g. operating costs), environmental (e.g. CO_2) or a combination of both. Scolan et al (2020) and Delubac et al (2021) developed a multi-period optimization tool to enhance the integration of solar thermal into district heating networks using a Mixed-Integer Non-Linear Programming (MINLP) approach. In their model, temperatures at the input and output of the solar field as well as mass flows are modeled as problem variables. Solar thermal power output is then computed based on global irradiance, ambient temperature, solar field temperature and DHN mass flows. As a result, thermo-hydraulic equations of the network are well modeled, thereby ensuring a comprehensive representation of the network, particularly regarding the impact influence of storage behavior on solar production. However, due to the large complexity and to avoid intractability issues, the MINLP problem is translated in NLP problem through the use of sigmoid functions, and representative days are used. The problem remains complex to solve and computationally expensive.

The other class of optimization problems is Mixed-Integer Linear Programming (MILP). MILP is commonly used for unit commitment problems to determine the optimal production plan for thermal plants to meet demand while minimizing costs or carbon emissions. In MILP models, mass flows and temperatures are treated as parameters rather than variables, as the thermo-hydraulic equations are linearized. This linearization enables the use of powerful linear solvers such as CPLEX, which provide stable solutions with guaranteed convergence, albeit with some approximations. Consequently, the model constraints in MILP are energy constraints like energy and power balances rather than temperature and flow rate balances. As a result, thermal solar production is often treated as a fixed input, computed solely based on solar radiation and solar field size (Buoro, 2014; Carpaneto 2015; Van Der Heijde, 2019). However, Lamaison et al (2018) highlighted the limitation of MILP models to get realistic trajectories noting that errors of several percent in the energy mix can arise, particularly due to oversimplification of storage modelling (i.e., the omission of temperature effects). Similarly, the oversimplification inherent in MILP models and neglecting temperature effects on plant performance can lead to an overestimation of solar production, as they fail to account for the impact of thermal storage, fluid inertia, and thermal losses in the solar field on overall system dynamics.

1.3. Aim of the paper

To address this gap, we propose a comprehensive six-step methodology designed to enhance the pre-calculation of solar thermal production for MILP optimization problems. By incorporating insights from the aforementioned studies, our methodology encompasses solar field and storage sizing, as well as a more precise computation of solar thermal production. Our methodology relies on efficient non-linear simulations with Modelica models and small optimization problems. The refined solar thermal production data can then be effectively utilized in classical MILP optimization problems for energy production, paving the way for more efficient and sustainable operation of Solar District Heating systems.

2. Methodology

The methodology is described in Figure 1 below and consists of six steps and an additional validation step.

- The first six steps represent the core of the methodology presented here. The objective is to improve the computation of solar thermal production by taking into account the behavior of thermal storage. It results in an improved thermal solar production trajectory Psol1.
- The six steps are based on Modelica models of increasing complexity (figure 2), alongside Python codes for sizing and optimization.
- The last 7th step involves a validation procedure. An iterative loop is established between a comprehensive Modelica model of the DHN plants, which generates a solar production profile called Psol[k]. This profile is then used in a MILP optimization model to determine optimal trajectories for biomass plant, gas plant and Pit Thermal Energy Storage (PTES). Convergence is assessed using the mean RMSE between two iterations Psol[k] and Psol[k+1].

- The inputs of the methodology are the external temperature, solar radiation, DHN temperatures and mass flow rate.
- The outputs are solar field area, pit thermal energy storage capacity and a more precise solar thermal power trajectory.

The different steps are detailed in the next subsections.

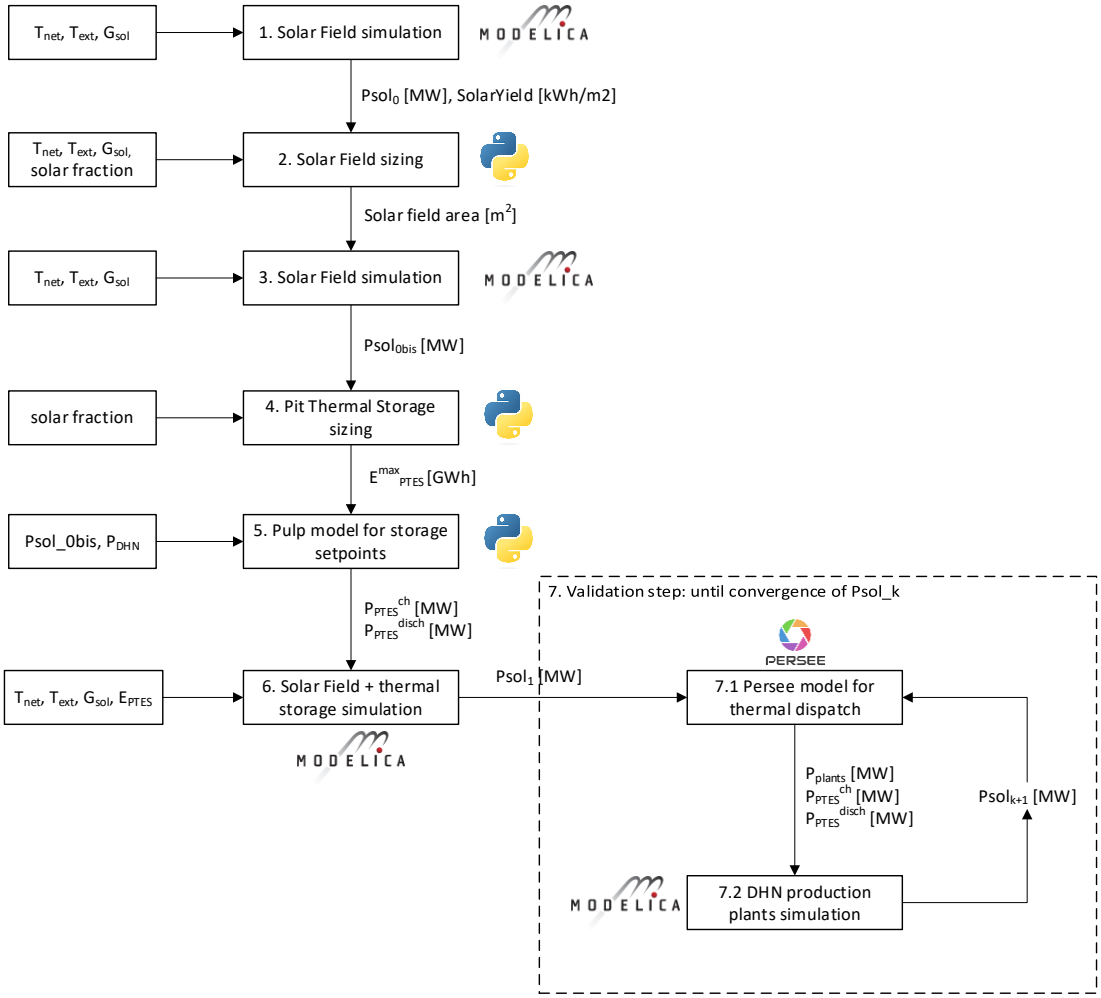

Figure 11- Methodology for precomputation of thermal solar production $Psol_1$ and validation procedures

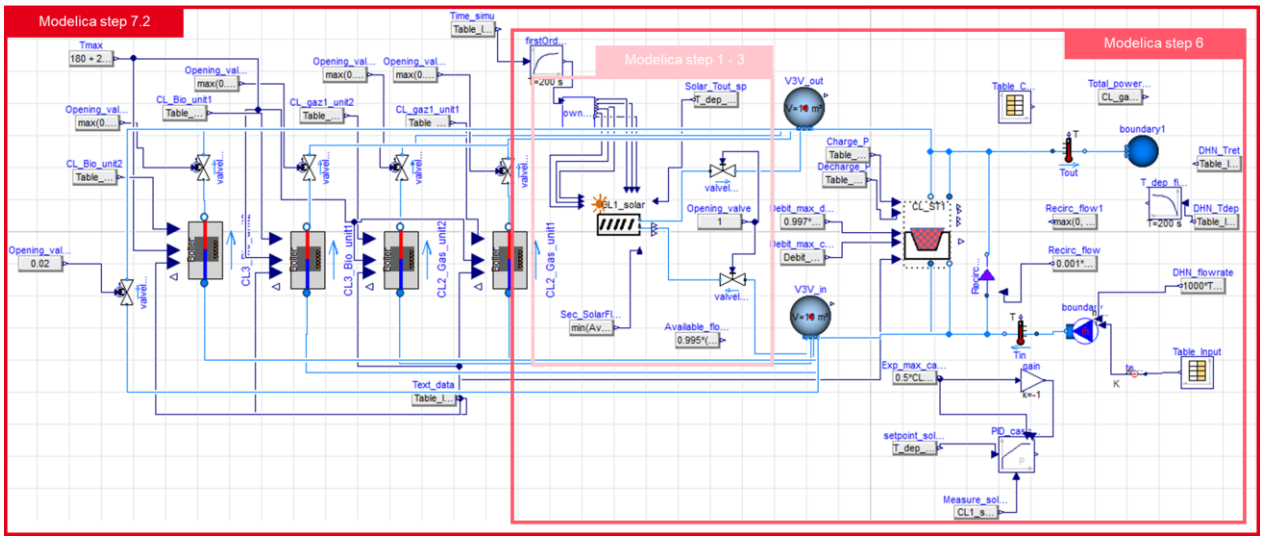

Figure 22 - Modelica models for step 1, 3, 5 and 7

2.1 Step 1: Solar field simulation for sizing

The first step involves a solar field Modelica model, developed using an in-house CEA Modelica library (Giraud, 2015). The objective of this simulation is to obtain a solar yield per unit area, in order to size the solar field to meet the system's solar energy requirements. The simulation is conducted using network temperature data (supply and return temperatures) and meteorological data (solar irradiation, ambient temperature). The simulation assumptions are the following:

- The return temperature of the network is set at the solar field heat exchanger secondary-side inlet.
- The solar field secondary flow rate is controlled to achieve the desired network supply temperature.
- The network flow rate is assumed to be unlimited so that all the energy from the solar field can be absorbed by the network

The outputs are time series of production in W/m² and annual $Solar\_yield$ in kWh/m²/year). The resulting time series here obtained is denoted $Psol_0$.

2.2. Step 2: Solar field sizing

The size of the solar field is computed by the following equation:

$$area\ [m^2] = SolarFraction[-] \cdot \frac{\sum_t P_{DHN}(t)[kWh]}{Solar\_yield\ [kWh/m^2]} \qquad (1)$$

Where $\sum_t P_{DHN}(t)$ is the DHN total annual energy and $Solar\_producible$ is the solar energy yield per unit area, obtained from step 1.

The solar fraction is a SDH parameter and is computed by $SolarFraction[-] = \frac{\sum_t P_{sol}(t)[kWh]}{\sum_t P_{DHN}(t)[kWh]}$ where Psol is the solar production.

2.3. Step 3: Solar field simulation

In large district heating networks where solar production constitutes a significant portion, the solar field may be extensive (potentially several thousands of square meters). In such cases, the impact of thermal loss and field inertia may not be neglected as it affects solar production. Therefore, the same Modelica model of step 1 is resimulated but with a corrected area and coherent pipe diameter, corresponding to the desired solar fraction.

It results in a new solar production called Psol_0bis.

After step 3, the simulation provides a solar production for a solar field corresponding to the required solar fraction within the network. The next step involves sizing the seasonal thermal energy storage (PTES) to achieve this solar fraction effectively.

2.4 Step 4: Pit storage sizing

Solar production exhibits high intermittency with significant variations between nights and days. Peak production can exceed DHN demand during several time steps, especially during summer. Thus, to meet the desired solar fraction (computed based on annual energy production), coupling solar field with Pit Thermal Energy Storage (PTES) is essential. The critical question is determining the appropriate capacity for this thermal energy storage.

The process is explained in Figure 3. This figure depicts the evolution of the cumulated difference between DHN demand and solar production $\sum_{s \le t} P_{DHN}(s) - P_{sol}(s)$. At the beginning of the year, solar production is lower than DHN demand, causing the cumulative difference to increase until the day T0. At T0, solar production surpasses DHN demand indicating a production surplus that should be stored. This production surplus continues until TF, where cumulative DHN demand exceeds again solar production.

Therefore, storage size corresponds to the difference of cumulative energy between T0 and TF, as depicted in the figure. This approach accounts for daily variations in PTES loading and unloading.

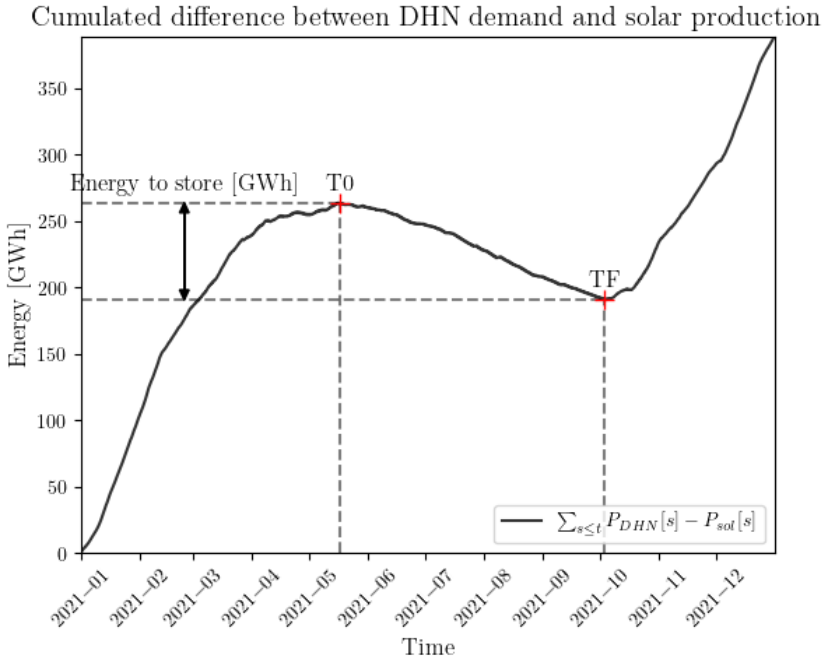

Figure 33 – Illustrative cumulated difference between P_{DHN} and P_{sol}

2.5 Step 5: MILP model for hypothetical charging and discharging profiles

The next step after PTES capacity design is to determine feasible charging and discharging profiles for the PTES. This is achieved through a small optimization problem formulated in PulP (Mitchell, 2011). The following assumptions to dispatch the energy are as follows:

- The charging power corresponds to the surplus of thermal solar production compared to DHN demand.
- The discharging power outside the period [T0-TF] should approximate a mean discharging value.

The optimization problem is the following (variables are shown in bold):

$$\min \sum_t \boldsymbol{\epsilon}^+[t] + \boldsymbol{\epsilon}^-[t] \qquad (2)$$

With the following constraints:

$$\boldsymbol{E}[0] = \boldsymbol{E}[T_{end}] \qquad (3)$$
$$\boldsymbol{E}[T0] = 0 \qquad (4)$$
$$\boldsymbol{E}[TF + 1] = E_{PTES}^{max} \qquad (5)$$

T0 and TF corresponds to the time steps where the storage is empty and fulfilled. These time steps are computed in step 2, simultaneously with the storage sizing.

From TF to T0, we want to approximate a mean discharging value :

$$\boldsymbol{P^{disch}}[t] = P_{mean}^{disch}[t] + \boldsymbol{\epsilon}^+[t] - \boldsymbol{\epsilon}^-[t] \qquad (6)$$

Where $\boldsymbol{\epsilon}^+$ and $\boldsymbol{\epsilon}^-$ represent deviations from the mean discharge value P_{mean}^{disch} which is computed from the following equation:

$$P_{mean}^{disch}[t] = \begin{cases} 0 \; when \; P^{ch}[t] > 0 \\ \frac{E^{max}}{\Delta t} \; else \end{cases} \qquad (7)$$

where Δt corresponds to the length of interval of time from TF to T0.

The discharging power must be less or equal to the DHN demand:

$$\boldsymbol{P^{disch}}[t] \leq P^{DHN}[t] \qquad (8)$$

Charging and discharging cannot occur simultaneously:

$$\boldsymbol{P^{disch}}[t] \cdot P^{ch}[t] = 0 \quad (9)$$

The energy balance of the storage is computed:

$$\boldsymbol{E}[t+1] - \boldsymbol{E}[t] = P^{ch}[t] - \boldsymbol{P^{disch}}[t] \quad (10)$$

The energy is the storage should remain positive within the storage capacity obtained in step 2:

$$\boldsymbol{E}[\boldsymbol{t}] \leq E_{PTES}^{max} \quad (11)$$

Note that we do not take into account thermal losses in the storage. The approach is to provide theoretical load profiles, matching with step-4 PTES sizing, close to a physical reality, rather than getting perfect loading and unload profiles matching the reality.

Solving this problem gives discharging profiles, close to a mean value during non-heating season. The optimization problem is linear, and does not involve any binary variables. A solution is then obtained in a few seconds.

2.6 Step 6: Simulation of a solar field model combined with thermal storage

After determining theoretical storage profiles, the next step is to assess the impact of these profiles on the solar field and overall district heating network. Therefore, a new Modelica model is developed, adapted from step 1 Modelica model including a PTES with loading/unloading setpoints and load-following thermal plant to meet DHN demand continuously. A simulation is performed with the following assumptions:

- The flow rate through the secondary side of the solar field heat exchanger is controlled in order to achieve the desired network supply temperature.
- The actual district heating network flow rates are considered.
- PTES operational setpoints (charge and discharge) from step 5 are used.

This new solar production is expected to be lower than Psol_0bis because of 1) the limited DHN mass flow (mass flow is no longer considered unlimited, and solar energy may need to be dissipated to prevent the solar field from overheating when the flow rate is restricted) and 2) the storage influence on the return temperature of the solar field heat exchanger when charging. Indeed, during PTES charging, network return temperature is mixed with PTES bottom temperature. The latter results in a higher temperature observed by the solar plant, compared to a simulation without storage. This can reduce the thermal solar output.

This simulation gives a new solar production Psol_1. The validity of this solar production is then assessed in an iterative loop between MILP optimization problem (to get optimal thermal plant trajectories satisfying heat demand) and a Modelica simulation model representing the whole district heating production plants.

2.7 Step 7: Validation

The validation step consists in an iterative loop and relies on two models:

- 7.1: a MILP optimization model based on the tool PERSEE (Ruby, 2024). This optimization model represents the district heating production plants, including the solar thermal plant and the PTES. Solar production $Psol_k$ is considered as fixed input profile. The objective is to satisfy heat demand while minimizing the operational costs. This step gives the production level plants P_{plants} and PTES profiles P_{PTES}^{ch} and P_{PTES}^{disch}.
- 7.2: A Modelica model representing the entire district heating production plants, including the solar field. The inputs are the production levels plants from PERSEE. This gives a revised solar production profile, noted $Psol_{k+1}$, k+1 corresponding to the $k+1^{th}$ iteration.

The convergence criteria is the mean root mean square difference between two iterations of Psol:

$$NRMSD = \frac{\sqrt{(\overline{Psol_k} - \overline{Psol_{k+1}})^2}}{\overline{Psol_k}} \quad (12)$$

The goal of this iterative loop is to align the production plant profiles with the solar production levels, thereby refining the optimization results to ensure they reflect a realistic and operationally feasible solar district heating system.

3. Results

3.1. Case study

The methodology presented here is applied on a hypothetical case study, representing a solar district heating network, with two different level of temperature (3rd and 4th generation district heating), with 3 different solar irradiances (corresponding to the meteorological areas H1, H2 and H3 in France). Network heat demand and supply/return temperatures are derived using the HeatPro tool (CEA Liten, 2024). The solar district heating network is composed of solar thermal plant, a pit thermal energy storage, biomass plants and gas plants. The desired solar fraction is 40%. (fig4)

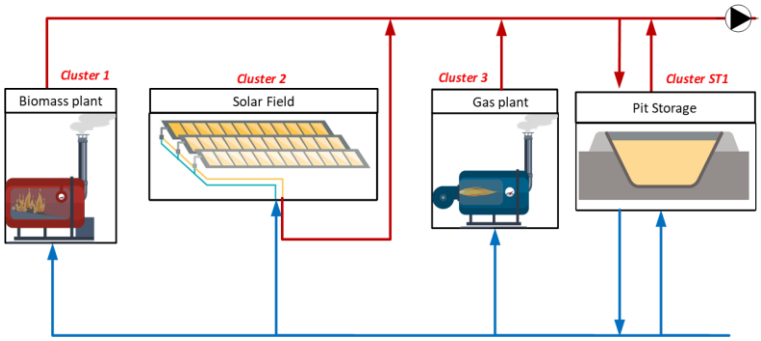

Figure 44 - DHN production plants

3.2. Solar precomputing production profile $Psol_1$

The following Table 1 presents the results of the precalculation methodology. It reports the difference between the corrected pre-calculated solar field production ($Psol_1$) with respect to the initial ideal simulation ($Psol_{0bis}$). It shows that $Psol_{0bis}$ overestimates the solar production level when storage is incorporated.

Table 1: Reduction in annual solar output between $Psol_{0bis}$ and P_{sol1} due to storage operation.

H1 3G	H1 4G	H2 3G	H2 4G	H3 3G	H3 4G
-11.6%	-10.8%	-11.3%	-10.5%	-7.4%	-8.3%

New solar fraction, recalculated using $Psol_1$ is shown in Table 2.

Table 2: Solar fraction computed with $Psol_1$. Desired solar fraction is 40%

H1 3G	H1 4G	H2 3G	H2 4G	H3 3G	H3 4G
35.3%	35.2%	35.7%	35.3%	36.7%	36.2%

As expected, solar fraction and annual solar output decrease when considering storage. This effect can be explained by Figure 5 representing the storage state of charge (right-axis) and the solar production $Psol_{0bis}$ (grey) and Psol1 (black) (left-axis). For clarity, solar production is represented as the maximum value over a one-week rolling window. As expected, solar production Psol1 is now lower than $Psol_{0bis}$. Several reasons can be identified:

- A limited mass flow of the solar field exchanger at the network side can lead to an overheating of the solar field, requiring to dissipate a part of the solar energy.
- At the beginning of the year, $Psol_1$ is lower than $Psol_{0bis}$ because of storage operation: PTES is discharging, thus limiting the mass flow available for the solar field. This limitation is more pronounced compared to $Psol_{0bis}$, which assumes unlimited mass flow rates to capture all potential solar production
- During summer, $Psol_1$ production levels are lower than $Psol_{0bis}$. This is also explained by storage operation: PTES is charging and its temperature is increasing. Thus, temperature observed by the solar field is higher than expected and solar production is reduced. This effect becomes even more pronounced at the end of summer when the storage is full.

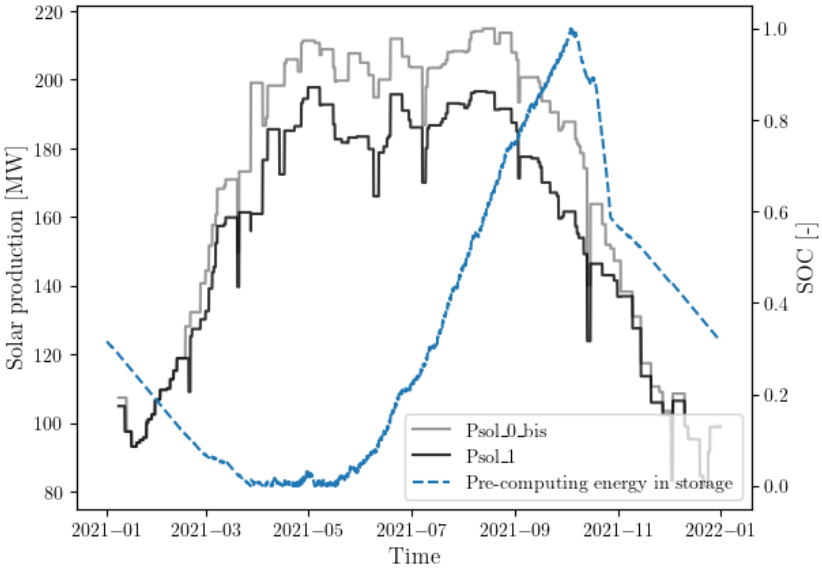

Figure 55 - Solar production and state of charge of H1 3G. Solar production is the max value over 1 week.

3.3. Validation step

Psol1 is generated using hypothetical storage profiles, which may not align with economically optimal profiles. To address this, an iterative loop between optimization and simulation is employed. PERSEE optimization model will generate optimal DHN plants trajectories to meet DHN demand over a year, with an hour time step precision. The objective function is the minimization of the operating costs. Then, Dymola simulation is conducted to generate actual solar production level when considering optimal discharging and charging profiles and the influence of other production plants. This iterative process not only refines the solar production profile but also highlights model mismatch between the simulation and optimization models. The validation loop is stopped after 6 iterations or if the convergence criteria (NRMSE) gets lower than 3%.

Figure 6 shows the RMSE evolution for the six different cases. Notably, for Montpellier 4G, NRMSE drops below 3% after three iterations at which point we consider that Psol has converged.

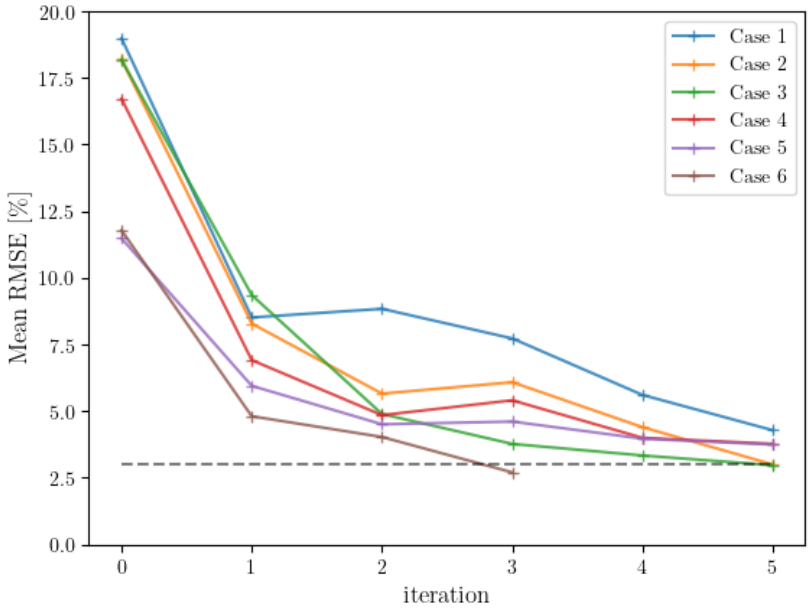

Figure 66 - Mean RMSE evolution

Throughout the iterative process, the solar production profiles gradually converge, as evidenced by the decreasing mean RMSE values across different iterations. The RMSE values, all of which are under 5%, indicate a high level of agreement between the optimization and simulation models. This suggests that the solar production profiles are becoming increasingly stable and consistent between these two models. However, perfect convergence is unattainable due to inherent model mismatches (e.g., different thermal loss models) and considering the fact that

MILP optimization can give multiple optimal solutions within an optimization gap (set here at 5%).

New solar fractions from solar production of the last iteration can be computed, presented in the Table 3.

Tab 3 - New solar fraction after convergence

H1 3G	H1 4G	H2 3G	H2 4G	H3 3G	H3 4G
36.5%	36.4%	37.2%	36.9%	37.8%	36.9%

New solar fractions are slightly higher than the ones obtained from Psol1 (they were around 35-36%). Actually the increase in solar production can be attributed to the modified storage behavior that results from considering economically optimal profiles.

Unlike in step 5 where only solar was able to be stored, step 7.1 considers the possibility of storing heat from biomass or gas plants (if it is economically profitable), which influences solar production profiles. As a result, charging and discharging profiles differs from those obtained in step5 (fig. 7). Storage is not used as expected and is maybe oversized as SOC in PERSEE (red continuous line) does not reach 1. In Psol1 (blue line), the storage is charged and discharged more frequently and for longer durations than in the full simulations. As a result, during charging periods, the maximum temperature is reached more quickly, thereby limiting solar production earlier ($Psol_1$). Additionally, with more frequent discharge periods, the flow rate is more often restricted, further limiting solar production. That explained the difference of solar production between Psol1 (black line) and Psol7 (the last iteration, red line), as seen in Figure 8.

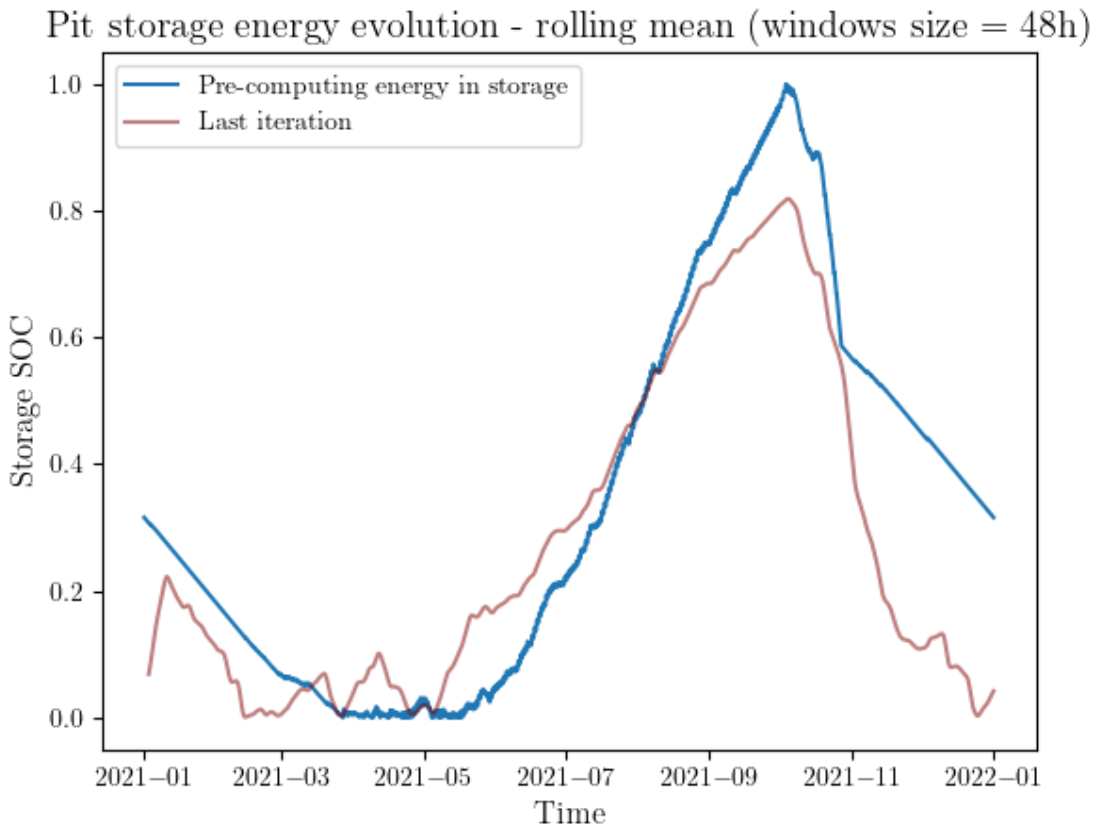

Figure 77 - Comparison of storage state of charge between Persee, Dymola and step 5 (H1 3G)

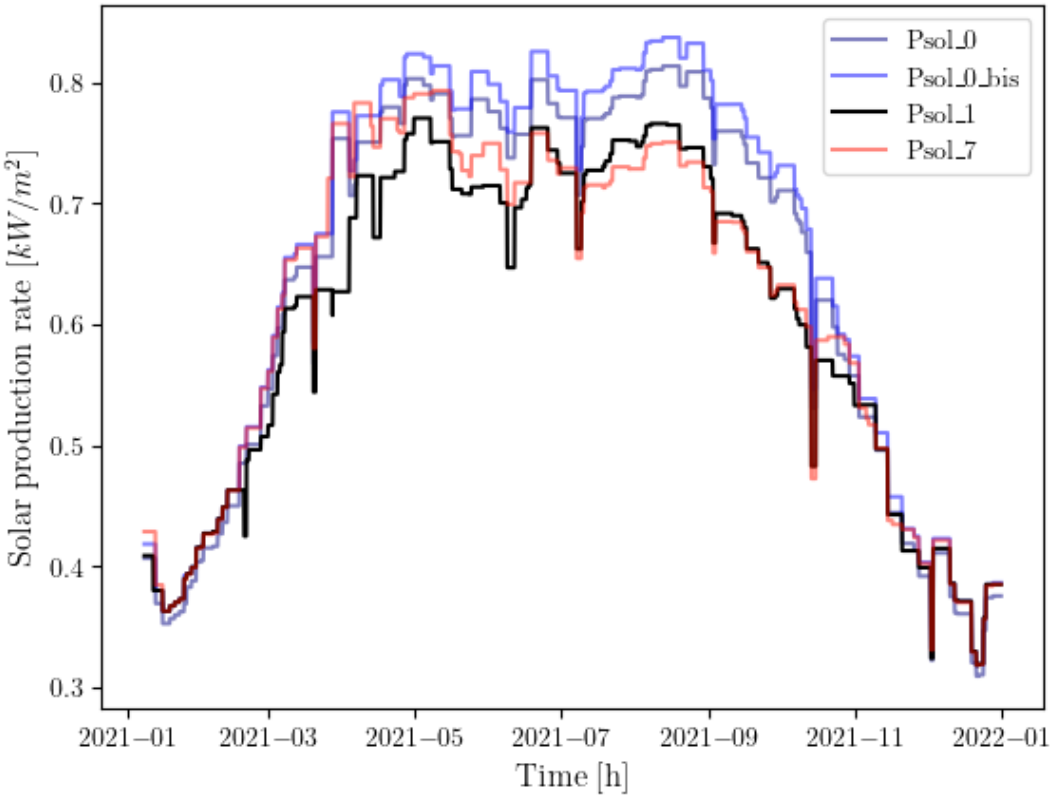

Figure 88 - Solar production rate in kW/m² for the first steps of the methodology and last iteration after convergence for H1 3G. Solar production is the max value over a week. (Solar production rate is shown to compare it with $Psol_0$ which is computed with a different surface)

Finally, Table 4 sums up the results and the difference on solar production and computation time for the methodology and the validation.

Table 4 - Methodology performance on precision and computation time

	H1 3G	**H1 4G**	**H2 3G**	**H2 4G**	**H3 3G**	**H3 4G**
$Esol_{0bis}$ [GWh]	260	252	200	192	137	134
$Esol_1$ [GWh]	230	225	177	172	127	123
Error on $Esol_{0bis}$ [%]	-11,6	-10,8	-11,4	-10,5	-7,4	-8,3
Esol after convergence [Gwh]	237	232	185	180	131	126
Error on $Esol_1$ [%]	3,26	3,30	4,25	4,33	3,12	2,06
Computation time : step 1->6 (sec)	418	394	374	369	348	383
Computation time: step 7 (sec)	7126	6100	4950	6069	7412	3322

While the average error between annual solar production of Psol1 (with estimated load profiles) and Psol0 (computation with solar field efficiency) was about -10%, the error between annual production of Psol1 and actual annual solar production after convergence is below 3.5%. However, the validation step is computationally intensive as it lasts from one hour to two hours, depending on the case. Moreover, the optimization step in PERSEE is costly, and we do not reach full optimality, the optimality gap was set at 5%. In contrast, steps 1 to 6 are very fast, with only few minutes to success 3 simulations (with simpler model than step 7.2) and an LP optimization. This seems to be a good compromise between accuracy and computational time for obtaining hourly solar production profiles and this within a methodology that is agnostic to other production sources.

4. Conclusion & perspectives

In conclusion, we present here a comprehensive methodology in order to enhance the pre-calculation of solar thermal production, particularly tailored for MILP-based optimization problems in Solar District Heating systems. By integrating solar field and pit thermal energy storage Modelica models with a LP optimization model for determining storage charging and discharging profiles, our approach offers a systematic framework for improving solar production pre-calculation levels.

These pre-calculated solar production levels are validated through a feedback loop utilizing in six different cases. Convergence between an optimization model (PERSEE), which fixed input solar thermal production to establish storage setpoints, and simulation models that account for the behavior of district heating plants and its influence on solar thermal production. After few iterations, our analysis revealed a final error rate of 3.4% between our pre-computed solar production and the actual solar production levels demonstrating the effectiveness of our methodology.

This method could be further refined to address model mismatches observed between the simulation and linear optimization, particularly in the representation of storage. Temperatures are not taken into account in MILP models, as a result, thermal losses are underestimated, and charging flow rates are overestimated. A potential solution could be to implement a rolling horizon approach within the validation loop. This approach would continuously update storage states in the optimization model based on non-linear simulation results, ensuring that charging flow rates and power outputs of other generators are more accurate as they are regularly updated by physical models. Consequently, the solar production calculated by Dymola would better account for the behaviors of other generators, leading to more precise results and fewer iterations in the validation loop. Such integration promises to refine the accuracy of our predictions and optimize system performance, thereby advancing the efficacy and sustainability of Solar District Heating systems

5. References

Brück, D., Elmqvist, H., Mattsson, S. E., & Olsson, H. (2002, March). Dymola for multi-engineering modeling and simulation. In Proceedings of modelica (Vol. 2002). Citeseer.

Buoro, D., Pinamonti, P., & Reini, M. (2014). Optimization of a distributed cogeneration system with solar district heating. Applied Energy, 124, 298-308.

Carpaneto, E., Lazzeroni, P., & Repetto, M. (2015). Optimal integration of solar energy in a district heating network. Renewable Energy, 75, 714-721.

CEA-Liten, District Heating load generator (2024). https://github.com/CEA-Liten/HeatPro [Access date 09-08-2024]

Descamps, M. N., Leoncini, G., Vallée, M., & Paulus, C. (2018). Performance assessment of a multi-source heat production system with storage for district heating. Energy Procedia, 149, 390-399.

Delubac, R., Serra, S., Sochard, S., Reneaume, J-M., 2021. A Dynamic Optimization Tool to Size and Operate Solar Thermal District Heating Networks Production Plants. Energies 14. 23, 8003

Giraud, Loïc & Bavière, R. & Paulus, Cédric. (2014). Modeling of solar district heating: a comparison between TRNSYS and MODELICA. 10.18086/eurosun.2014.19.06.

Giraud, L., Baviere, R., Vallée, M., & Paulus, C. (2015, September). Presentation, validation and application of the DistrictHeating Modelica library. In Proceedings of the 11th International Modelica Conference (Vol. 118, pp. 79-88). Linköping, Sweden: Linköping University Electronic Press.

Lamaison, N., Collette, S., Vallée, M., & Bavière, R. (2019). Storage influence in a combined biomass and power-to-heat district heating production plant. Energy, 186, 115714.

Lund, H., Werner, S., Wiltshire, R., Svendsen, S., Thorsen, J. E., Hvelplund, F., & Mathiesen, B. V. (2014). 4th Generation District Heating (4GDH): Integrating smart thermal grids into future sustainable energy systems. Energy, 68, 1-11.

Mitchell, S., OSullivan, M., & Dunning, I. (2011). Pulp: a linear programming toolkit for python. The University of Auckland, Auckland, New Zealand, 65, 25.

Renaldi, R., & Friedrich, D. (2019). Techno-economic analysis of a solar district heating system with seasonal thermal storage in the UK. Applied Energy, 236, 388-400.

Ruby, A., Crevon, S., Parmentier, P., Gaoua, Y., Lavialle, G. (2024). Persee, a single tool for various optimizations of multi-carrier energy system sizing and operation. In ECOS 2024-Efficiency, Cost, Optimization and Simulation of energy conversion systems and processes.

Saloux, E., & Candanedo, J. A. (2021). Model-based predictive control to minimize primary energy use in a solar district heating system with seasonal thermal energy storage. Applied energy, 291, 116840.

Salvestroni, M., Pierucci, G., Pourreza, A., Fagioli, F., Taddei, F., Messeri, M., & De Lucia, M. (2021). Design of a solar district heating system with seasonal storage in Italy. Applied Thermal Engineering, 197, 117438.

Scolan, S., Serra, S., Sochard, S., Delmas, P., & Reneaume, J. M. (2020). Dynamic optimization of the operation of a solar thermal plant. Solar Energy, 198, 643-657.

University of Wisconsin--Madison. Solar Energy Laboratory. (1975). TRNSYS, a transient simulation program. Madison, Wis. :The Laboratory,

Van Der Heijde, B., Vandermeulen, A., Salenbien, R., & Helsen, L. (2019). Representative days selection for district energy system optimisation: a solar district heating system with seasonal storage. Applied Energy, 248, 79-94.